Fatigue life of specimens with round and rectangular cross-sections under out-of-phase bending and torsional loading

D. Rozumek, Z. Marciniak and E. Macha

Opole University of Technology, Faculty of Mechanical Engineering, Mikołajczyka 5, 45-271 Opole, Poland, e-mail address: d.rozumek@po.opole.pl

ABSTRACT. *The paper contains the fatigue test results of specimens with rectangular and round cross-sections, made of 10HNAP (S355J2G1W) steel. The rectangular specimen height to width ratio was 1.5. The tests under cyclic bending with torsion were carried out for the following ratios of normal to shear stresses amplitudes* $\sigma_a / \tau_a = 0.5$, *1, 2 and the loading frequency was 26.5 Hz. Nominal stresses were chosen for the equivalent stress amplitude according to the Huber-Mises hypothesis equal to 360 MPa. Unilaterally restrained specimens were subjected to bending with torsion for different nominal normal stresses* σ_a *= 99, 180, 272 MPa and the nominal shear stresses* τ_a *= 136, 180, 199 MPa to the crack initiation. The tests were performed in the high cycle fatigue regime for the stress ratio R = - 1 and phase shift between bending and torsion equal to* $\phi = 0^\circ$ *and* 90°.

INTRODUCTION

Bending with torsion often occurs [1, 2] in machine elements such as shafts [3, 4] or beams [5] applied in many fields of industry. Round specimens are usually subjected to fatigue tests of materials under combined bending with torsion, while other sections are not so often tested. Non-zero gradients of normal σ and shear τ stresses occur under such biaxial loading. During fatigue life calculations it is necessary to reduce the multiaxial stress state to the uniaxial one (usually corresponding to bending), so the fatigue failure criteria must be applied. They can be divided into stress, strain and energy based criteria. The most often applied and verified criteria are the following:
(i) the stress criteria proposed by Gough and Pollard [6], Nishihara-Kawamoto [7], Findley [8], McDiarmid [9], Zenner et al. [10], Macha [11], Dang Van [12], Sonsino [13], Papadopoulos [14],
(ii) the strain criteria formulated by Brown and Miller [15], Lohr and Ellison [16], Socie et al. [17], Bantachfine et al. [18],
(iii) the energy criteria proposed by Liu [19], Varvani-Farahani [20], Ellyin et al. [21], Chen et al. [22], Łagoda and Macha [23] and other [24].

Only some of these criteria were considered under non-proportional loadings. Their usability in fatigue life calculations is evaluated together with the chosen hypothesis of

damage accumulation, and the calculated fatigue life N_{cal} is compared with the experimental one N_{exp}.

The aim of this paper is to compare the calculated fatigue lives with experimental ones obtained from tests under proportional and nonproportional bending to torsion with different amplitude ratios and two different cross-sections of specimens made of 10HNAP steel.

EXPERIMENTS

For fatigue test were selected specimens with rectangular (area 42.2 mm^2) and round (area 50.3 mm^2) cross-sections, made of 10HNAP (S355J2G1W) constructional steel. The material is a low-alloy of higher resistance to atmospheric corrosion structural steel. Figure 1 shows a shape and dimensions of specimens. They were cut from the sheets 16 mm in thickness according to the rolling direction. The specimen surfaces were ground and polished. The used steel is weldable, in improved state; its chemical composition and mechanical properties are presented in Tables 1 and 2. The test results presented in this paper were obtained in Department of Mechanics and Machine Design, Opole University of Technology. The tests were carried out at the test stand MZGS-100Ph (Fig. 2). This machine allows to realize cyclic bending with torsion and phase displacement between the bending moment and torsional moment in the range $0 \div 180°$ [5]. The tests were realized under loading with the controlled force (in the considered case, the moment amplitude was controlled) and loading frequency 26.5 Hz. The fatigue tests were performed for a high number of cycles under the stress ratio $R = -1$.

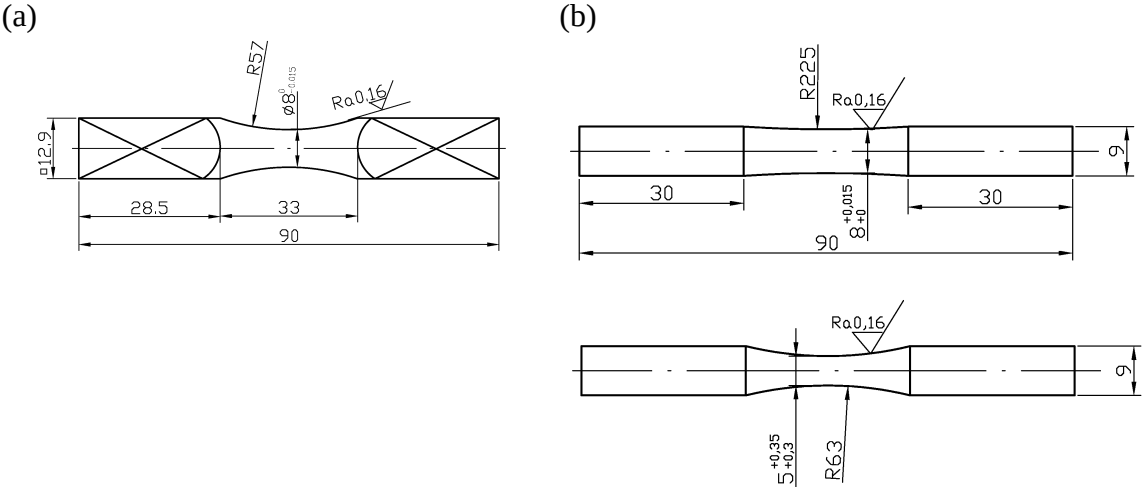

Figure 1. Shape and dimensions of specimens with: (a) round cross-section and (b) rectangular cross-section, dimensions in mm

Table 1. Chemical composition of 10HNAP steel in %

C	Mn	Si	P	S	Cr	Ni	Cu	Fe
0.11	0.52	0.26	0.098	0.016	0.65	0.35	0.26	Bal.

Table 2. Mechanical properties of 10HNAP steel

Yield stress σ_{YS} (MPa)	Ultimate stress σ_U (MPa)	Elastic modulus E (GPa)	Poisson`s ratio ν	σ_{af} (MPa)	N_f (cycles)
418	566	215	0.29	300	$3 \cdot 10^6$

The tests were carried out for different amplitudes of bending moments M_{Ba} = 5.64, 10.17, 15.38 N·m and torsional moments M_{Ta} = 8.23, 10.89, 12.08 N·m, corresponding to the nominal amplitudes of normal stresses σ_a = 99, 180, 272 MPa (in case of rectangular cross-section at the middle of shorter specimen sides 5.3 mm) and the nominal amplitudes of shear stresses τ_a = 136, 180, 199 MPa to the crack initiation. The tests under bending with torsion were realized for the ratio M_{Ba} / M_{Ta} = 0.47, 0.94, 1.87 (Fig. 3). Loadings were selected for the following amplitude ratios of normal to shear stresses: σ_a / τ_a = 0.5, 1 and 2. The tests were realized under simultaneous bending with torsion (in phase - $\phi = 0°$ and out of phase - $\phi = 90°$).

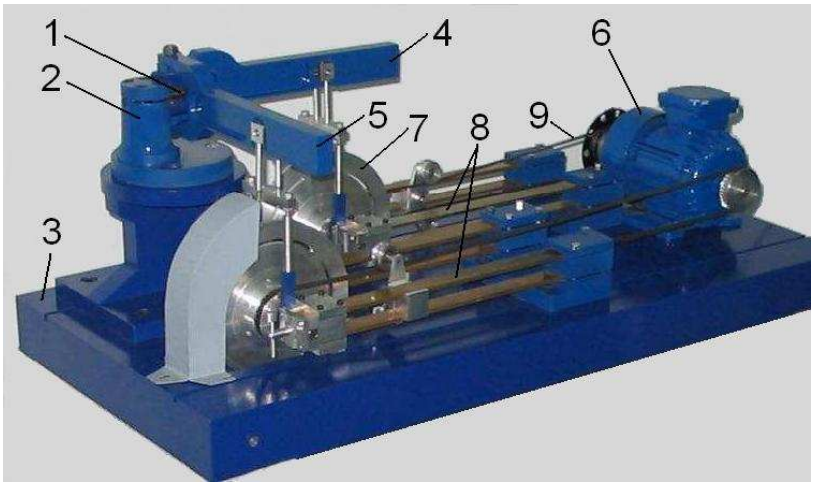

Figure 2. The fatigue test stand MZGS-100Ph: 1 –specimen, 2 – head, 3 – base of the machine, 4 – bending lever, 5 – torsional lever, 6 – motor, 7- rotating disk, 8 – plane springs, 9 – strip

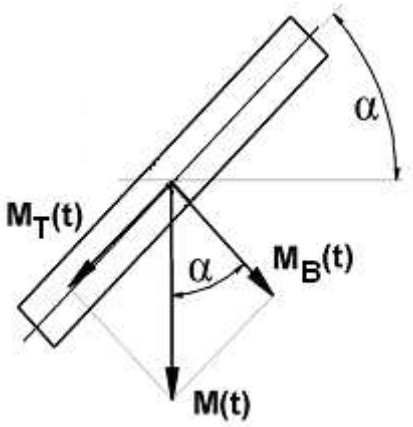

Figure 3. Scheme of the specimen loading

THE TEST RESULTS AND THEIR ANALYSIS

The tests allowed to determine a number of cycles N_f to the fatigue crack initiation. From the test results it arises (Fig. 4) that higher fatigue lives appear for specimens with rectangular cross-sections for all combinations of bending with torsion and phase shifts ϕ. Fatigue life N_f of round specimens for phase shift $\phi = 90^o$ is greater than for $\phi = 0°$ for all the considered stress amplitude ratios. Such tendency of N_f variation is not observed in rectangular specimens. In specimens with rectangular cross-section under the same amplitude loading and $\phi = 0°$ ($\sigma_a = 0.5\tau_a$ and $\sigma_a = \tau_a$) as well as $\phi = 90^o$ ($\sigma_a = 0.5\tau_a$), two different lives were found. Six specimens in each series were tested. Different lives were a result of different initiations of crack paths. In one case, fatigue crack growth was observed at the lateral surfaces from both sides the top and the bottom. Here, lower lives were recorded ($\sigma_a = 0.5\tau_a$, $\sigma_a = \tau_a$ and $\phi = 0°$, $\sigma_a = 0.5\tau_a$ and $\phi = 90°$). In the other case, the crack growth was observed at the lateral surfaces only from the top or from the bottom, and then higher lives were recorded ($\sigma_a = 0.5\tau_a$, $\sigma_a = \tau_a$ and $\phi = 0°$, $\sigma_a = 0.5\tau_a$ and $\phi = 90°$).

The tests were performed in order to verify the fatigue criteria by Gough-Pollard [6], the modified criterion by Huber-Mises [25], the modified criterion by Tresca-Guest [25] and Nishihara-Kawamoto [7].

Fig. 5 shows relations between the shear stress amplitude τ_a and the normal stress amplitude σ_a for the tested round cross-section specimens and two different numbers of cycles to failure for $\phi = 0°$.

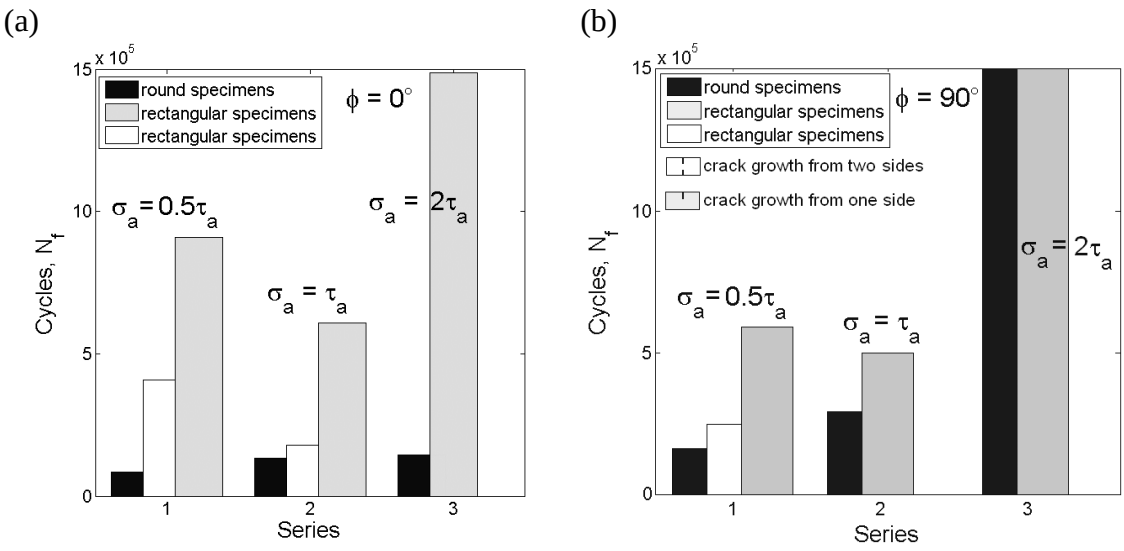

Figure 4. Comparison of mean fatigue lives for specimens with round and rectangular cross-sections and phase shift between bending and torsional loading equal to: (a) $\phi = 0°$ and (b) $\phi = 90°$

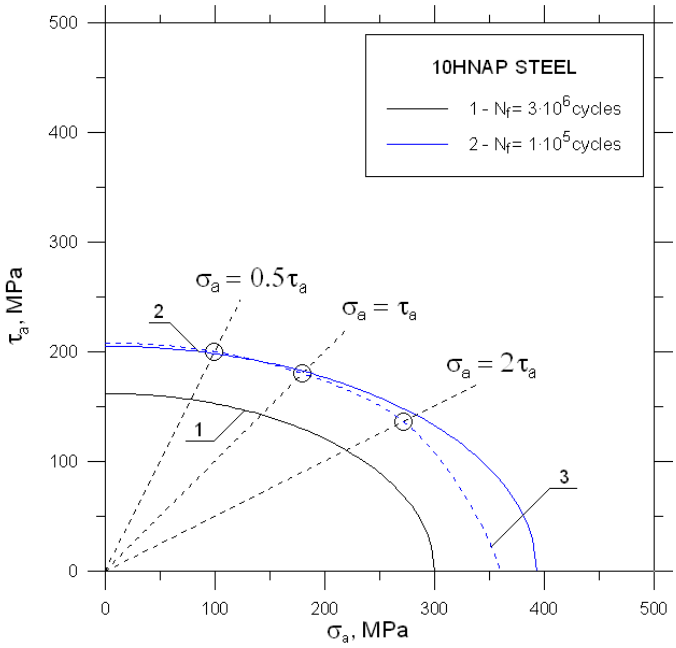

Figure 5. Limit state in round cross-section specimens for two numbers of cycles to failure N_f under bending and torsion $\phi = 0°$

Graph 1 in Fig. 5 shows the Gough-Pollard model (ellipse quadrant) describing the limit state for $N_f = 3 \cdot 10^6$ cycles, and solid line 2 is the curve for $N_f = 1 \cdot 10^5$ cycles. Broken

line 3 is related to the equivalent stress equal to 360 MPa, obtained according to the Huber-Mises hypothesis for different ratios of normal and shear stresses.
The curve 1 can be described by the equation (in MPa), which takes the following form at the fatigue strength for $N_f = 3 \cdot 10^6$ cycles

$$\left(\frac{\sigma_a}{300}\right)^2 + \left(\frac{\tau_a}{162}\right)^2 = 1 \tag{1}$$

From Fig. 5 it appears that there is a good conformity of test results for the verified combinations of bending and torsion with the Gough-Pollard curve for $N_f = 1 \cdot 10^5$ cycles.
The equivalent stresses according to the considered criteria are as follows:
- the modified Huber-Mises criterion (mode H-M) [25]

$$\sigma_{eq} = \frac{\sigma_a}{\sqrt{2}} \sqrt{1 + \frac{3}{4}\left(\frac{2\tau_a}{\sigma_a}\right)^2 + \sqrt{1 + \frac{3}{2}\left(\frac{2\tau_a}{\sigma_a}\right)^2 \cos(2\phi) + 0.5625\left(\frac{2\tau_a}{\sigma_a}\right)^4}}, \tag{2}$$

- the modified Tresca-Guest criterion (mode T-G) [25]

$$\sigma_{eq} = \frac{\sigma_a}{\sqrt{2}} \sqrt{1 + \left(\frac{2\tau_a}{\sigma_a}\right)^2 + \sqrt{1 + 2\left(\frac{2\tau_a}{\sigma_a}\right)^2 \cos(2\phi) + \left(\frac{2\tau_a}{\sigma_a}\right)^4}}, \tag{3}$$

- the Nishihara-Kawamoto criterion (N-K) [7]
for $\phi = 0°$

$$\sigma_{eq} = \frac{\sqrt{\left(k^2 + 1\right)\sigma^2{}_a + \left(3 - k^2\right)\sigma_a \sqrt{\sigma_a^2 + 4\tau_a^2} + 4\tau_a^2 k^2}}{2}, \tag{4}$$

for $\phi = 90°$

$$\sigma_{eq} = \sqrt{\frac{4\sigma_a^2 + \beta\left(\left(1 + k^2\right)\sigma_a^2 + \left(3 - k^2\right)\sigma_a \sqrt{\sigma_a^2 + 4\tau_a^2} + 4\tau_a^2 k^2\right)}{4(1 + \beta)}}. \tag{5}$$

where: $k = \frac{\sigma_{af}}{\tau_{af}} \geq \sqrt{3}$ - limit ratio (for calculation assumed $\sigma_{af} / \tau_{af} = 1.85$), $\beta = 1$ – coefficient of sensitivity for loading phase shift.
The lives N_{cal} shown in Figs. 6-11 were calculated from Eqs. (2) – (5) and compared with the experimental lives N_{exp}. Figs. 6-8 present comparison of N_{cal} and N_{exp} for

specimens with round and rectangular cross-sections, phase shift $\phi = 0°$ and various stresses amplitude ratios $\sigma_a = 0.5\tau_a$, $\sigma_a = \tau_a$, $\sigma_a = 2\tau_a$. The solid line means ideal conformity between N_{cal} and N_{exp}, and the broken lines present the result scatter bands of coefficients $N_{cal} / N_{exp} = 3$ (1/3).

From Figs. 6a – 11a for round specimens it appears that the fatigue lives N_{cal} calculated according to the modified Tresca-Guest criterion (3) are the most similar to the experimental lives N_{exp} and they are included into the scatter band of coefficient 3 for all the applied amplitude ratios and stress phase shifts. However the calculated lives N_{cal} of rectangular specimens (Figs. 6b – 11b) for both phase shifts angles and stress amplitude ratios (except for $\sigma_a = 2\tau_a$ in Fig. 8b) are included into the scatter band of coefficient 3 and they are the most similar to the experimental lives N_{exp}, if the calculations are performed according to the modified Huber-Mises criterion (2). Let us note that N_{cal} (under $\sigma_a = 2\tau_a$ and $\phi = 0°$) according to Eq. (2) in Fig. 8b is located at the safe side, i.e. outside the scatter band of coefficient 3 its value is more than 3 times greater than the real fatigue life of the specimen N_{exp}.

In Figs. 6b, 7b and 9b for rectangular specimens two experimental lives can be observed. It is caused by various developments of cracks in the specimens. In the specimens of lower life the fatigue cracks developed at both sides of the specimen (white marks), and in the case of higher lives the cracks developed at one side (grey marks). In Fig. 11b unlimited life is obtained for rectangular specimens.

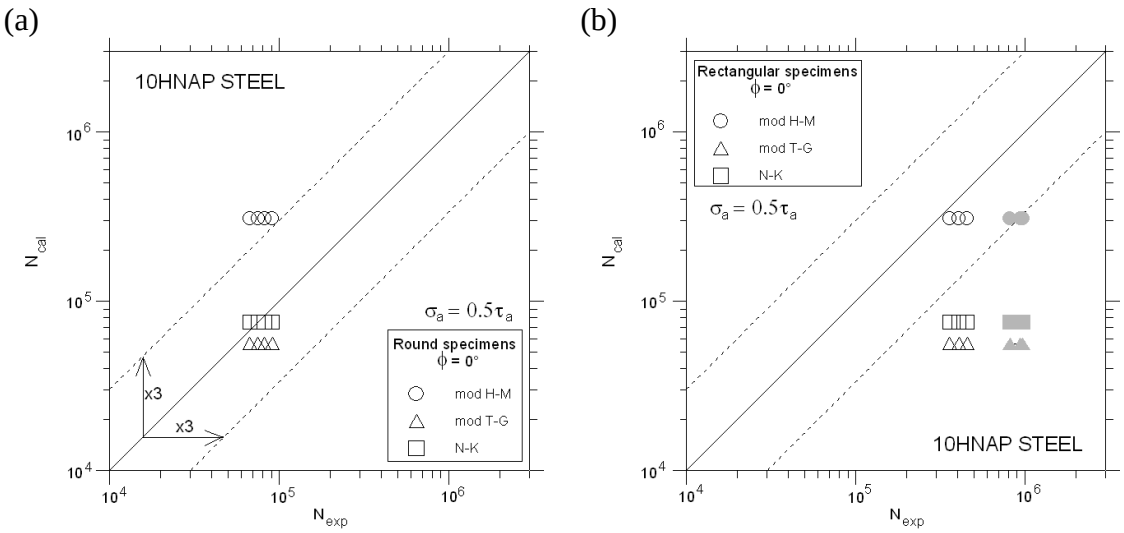

Figure 6. Comparison of fatigue lives of specimens with: (a) round and (b) rectangular cross-sections obtained from calculations N_{cal} and experiments N_{exp} for phase shift $\phi = 0°$, and stress amplitudes $\sigma_a = 0.5\tau_a$

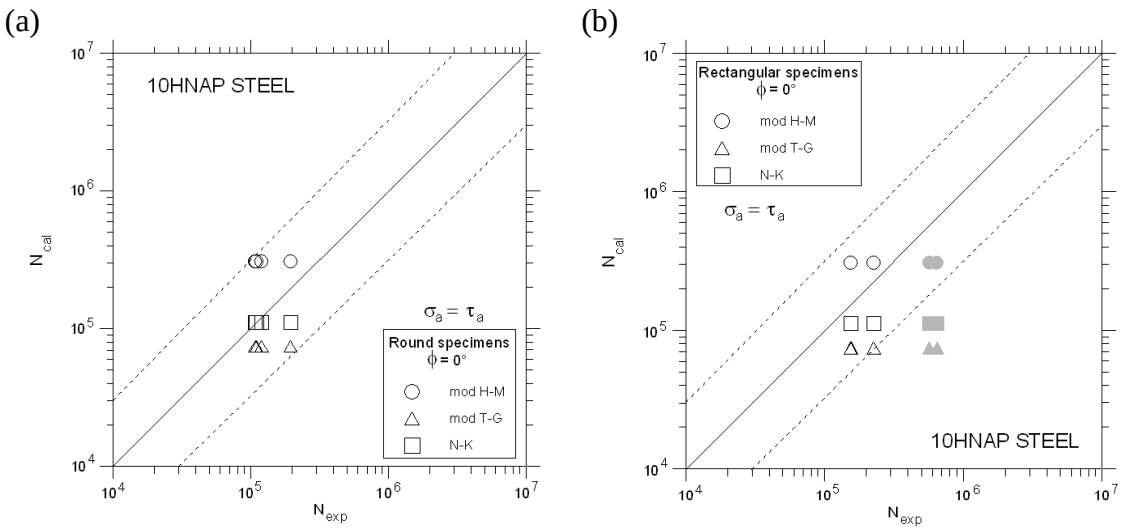

Figure 7. Comparison of fatigue lives of specimens with: (a) round and (b) rectangular cross-sections obtained from calculations N_{cal} and experiments N_{exp} for phase shift $\phi = 0°$, and stress amplitudes $\sigma_a = \tau_a$

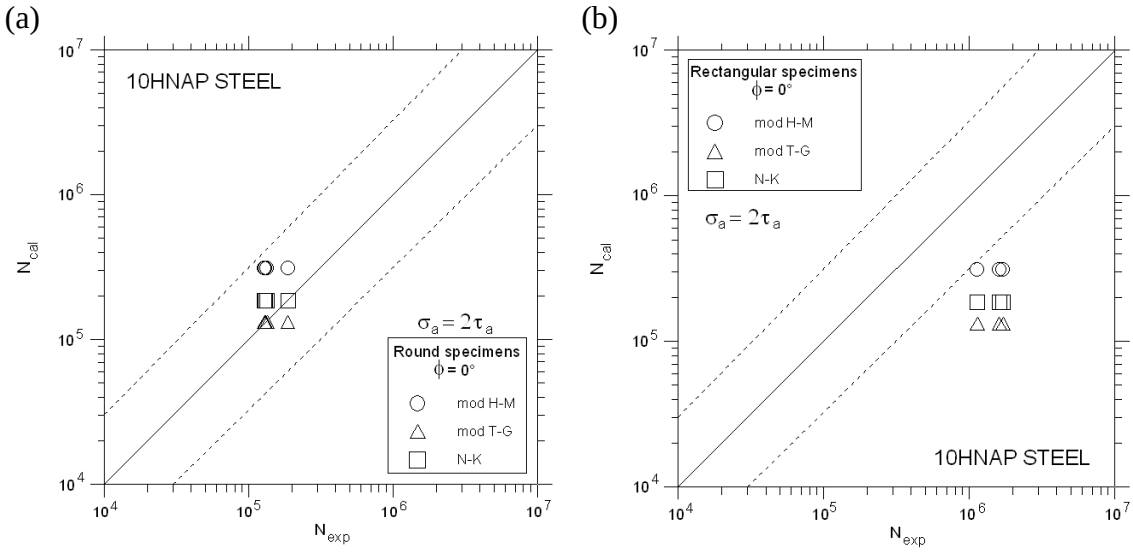

Figure 8. Comparison of fatigue lives of specimens with: (a) round and (b) rectangular cross-sections obtained from calculations N_{cal} and experiments N_{exp} for phase shift $\phi = 0°$, and stress amplitudes $\sigma_a = 2\tau_a$

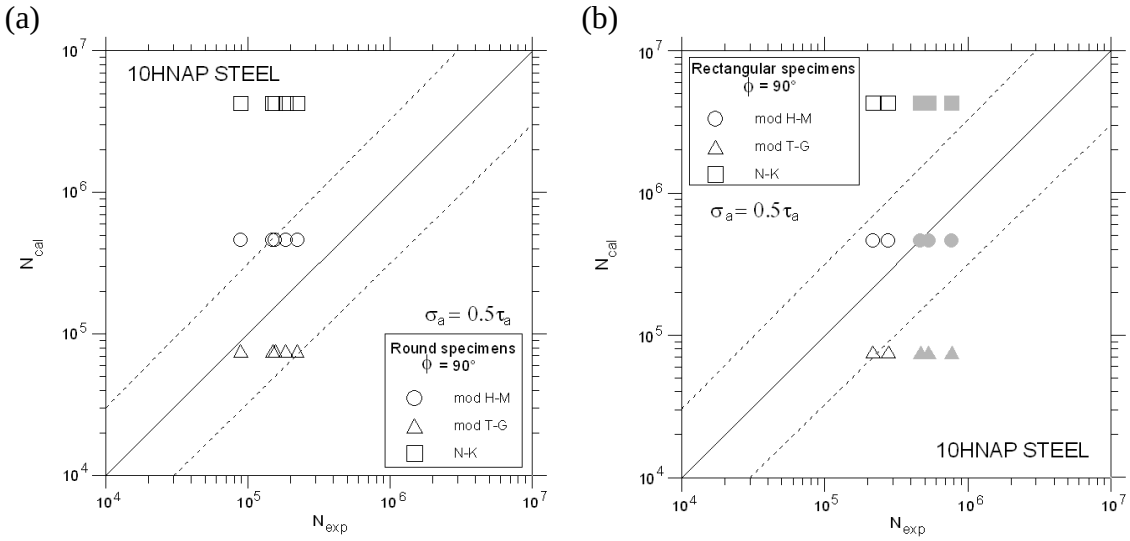

Figure 9. Comparison of fatigue lives of specimens with: (a) round and (b) rectangular cross-sections obtained from calculations N_{cal} and experiments N_{exp} for phase shift $\phi = 90°$, and stress amplitudes $\sigma_a = 0.5\tau_a$

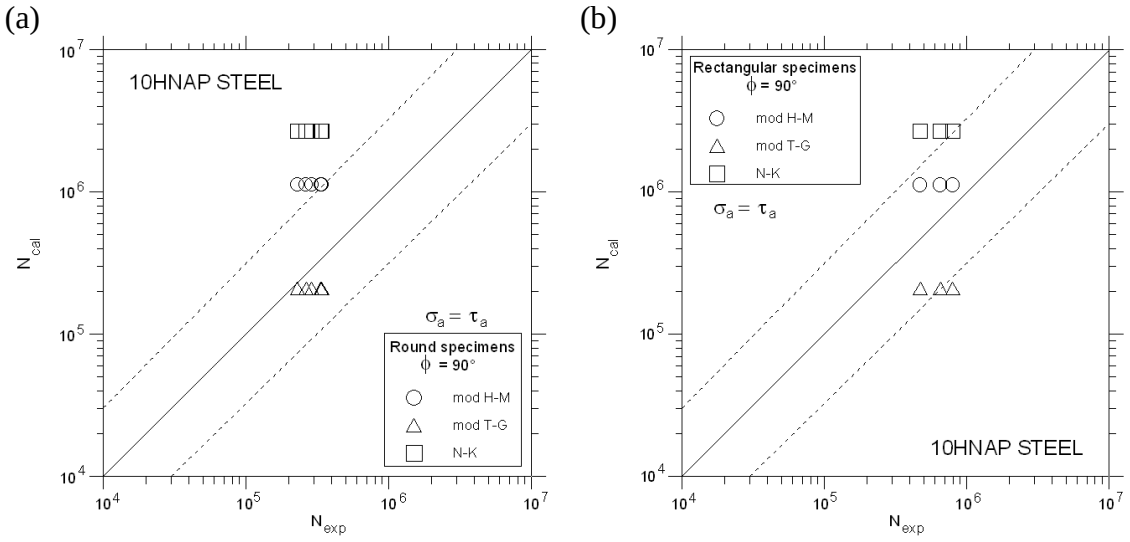

Figure 10. Comparison of fatigue lives of specimens with: (a) round and (b) rectangular cross-sections obtained from calculations N_{cal} and experiments N_{exp} for phase shift $\phi = 90°$, and stress amplitudes $\sigma_a = \tau_a$

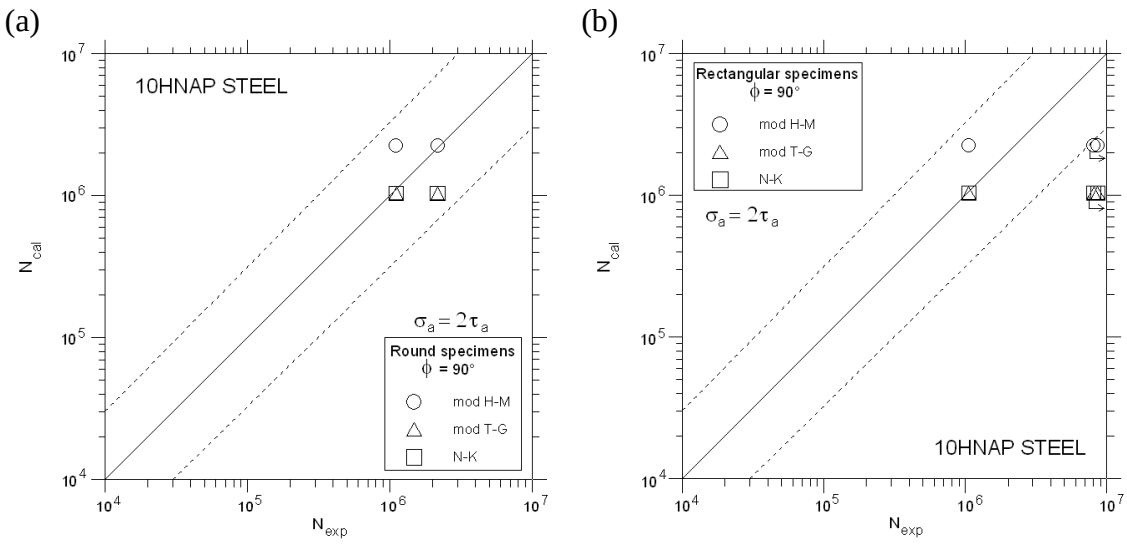

Figure 11. Comparison of fatigue lives of specimens with: (a) round and (b) rectangular cross-sections obtained from calculations N_{cal} and experiments N_{exp} for phase shift $\phi = 90°$, and stress amplitudes $\sigma_a = 2\tau_a$

CONCLUSIONS

Basing on the calculated and experimental fatigue lives for the tested 10HNAP steel, following conclusions can be formulated:

1. The fatigue lives of round specimens calculated according to the modified Tresca-Guest criterion are the most similar to the experimental lives and they are included into the scatter band of coefficient 3 for all the applied amplitude ratios and stress phase shifts.
2. Satisfactory conformity of calculated and experimental fatigue lives was observed for rectangular cross-sections specimens when the modified Huber-Mises criterion was applied.
3. In rectangular specimens with phase shift $\phi = 0°$ ($\sigma_a = 0.5\tau_a$, $\sigma_a = \tau_a$) and $\phi = 90°$ ($\sigma_a = 0.5\tau_a$) two fatigue lives be found. It results from different sides of fatigue crack initiation.
4. In the case of phase shift change from 0° to 90° we can found fatigue life increase for round cross-sections specimens and all stress ratios.
5. In the case of stresses amplitude ratios $\sigma_a / \tau_a = 0.5$, 1, 2 and $\phi = 0°$ and 90° for round and rectangular sections we can observe fatigue life increase, except rectangular sections with ($\phi = 0°$) and $\sigma_a / \tau_a = 1$, where fatigue life decrease occurs.

Acknowledgements
This work was supported by the National Centre for Research and Development, contract No. N R03 0065.

REFERENCES

1. Xia Z., Ellyin F. (1998) *Int. J. Fatigue* **20**, 51-56.
2. Findley WN. (1959) *Journal of Engineering for Industry*, 301-306.
3. Sonsino CM., Grubisic (1989). In: *Biaxial and Multiaxial Fatigue*, pp. 335-353, Brown M.W. and Miller K.J. (Eds), Mechanical Engineering Publications.
4. Marciniak Z., Rozumek D. & Macha E. (2008) *Int. J. of Fatigue* **30**, 800-813.
5. Rozumek D., Marciniak Z. (2009) *Przegląd Mechaniczny* **2**, 15-19.
6. Gough H.J., Pollard H.V. (1935). Institution of Mechanical Engineers, pp. 549-573.
7. Nishihara T., Kawamoto M. (1945). Memoirs of the College of Engineering, pp. 85-112, Kyoto Imperial University, Japan.
8. Findley W. N. (1959) *Journal of Engineering for Industry*, 301-306.
9. McDiarmid D. L. (1987) *Fatigue Fract. Engng Mater. Struct.* **9**, 457-475.
10. Zenner H., Simbürger A., Liu J. (2000) *Int. Journal of Fatigue* **22**, 137-145.
11. Macha E. (1989). In: *Biaxial and Multiaxial Fatigue*, pp. 425-436, Brown M.W. and Miller K.J. (Eds), Mechanical Engineering Publications.
12. Dang Van K., Griveau B., Message O. (1989). In: *Biaxial and Multiaxial Fatigue*, pp. 479-496, Brown M.W. and Miller K.J. (Eds), Mechanical Engineering Publications.
13. Sonsino C.M., Grubisic V. (1987) *Werkstofftech*, **18**, 55-70.
14. Papadopoulos I.V. (1994) *Int. J. Fatigue*, **16**, 377-384.
15. Brown M. W., Miller K. J. (1973). Institution of Mechanical Engineers, pp. 745-755.
16. Lohr R.D., Ellison E.G. (1980) *Fatigue of Engineering Materials and Structures*, **3**, 1-17.
17. Socie D. (1993) *ASTM STP 1191*, 7-36.
18. Bantachfine S., Azari Z., Pluvinage G, Toth L. (1996) *Engineering Fracture Mechanics*, **54**, 513-522.
19. Liu K.C. (1993) *ASTM STP 1191*, 67-84.
20. Varvani–Farahani A. (2000) *Int. J. Fatigue*, **22**, 295-305.
21. Ellyin F., Gołoś K., Xia Z. (1991) *J. Enging. Mater. Technol. ASME*, **113**, 112-118.
22. Chen X., Xu S., Huang D. (1999) *Fatigue Fract. Engng Mater. Stuct.*, **22**, 679-686.
23. Łagoda T., Macha E, Morel F., Niesłony A. (2001). In: Conference on Biaxial/Multiaxial Fatigue and Fracture, pp. 233-240, de Freitas M. (Ed.), Instituto Superior Técnico.
24. Macha E. (2001) *The Archive of Mechanical Engineering*, **XLXIII**, 71-101.
25. SAE Fatigue Design Handbook (1997) *Society of Automative Engineers*, 470.